INFLUENCE OF A RIGID TOP MASS ON THE RESPONSE OF A PRESSURIZED CYLINDER CONTAINING LIQUID

by

Daniel D. Kana
Wen-Hwa Chu

FINAL REPORT, PART I
Contract No. NAS8-21282
Control No. DCN 1-8-75-00009 (1F)

SwRI Project No. 02-2332

Prepared for

National Aeronautics and Space Administration
George C. Marshall Space Flight Center
Huntsville, Alabama

2 June 1969

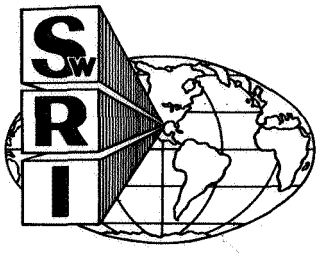

SOUTHWEST RESEARCH INSTITUTE
SAN ANTONIO HOUSTON

SOUTHWEST RESEARCH INSTITUTE
Post Office Drawer 28510, 8500 Culebra Road
San Antonio, Texas 78228

INFLUENCE OF A RIGID TOP MASS ON THE RESPONSE OF A PRESSURIZED CYLINDER CONTAINING LIQUID

by

Daniel D. Kana
Wen-Hwa Chu

FINAL REPORT, PART I
Contract No. NAS8-21282
Control No. DCN 1-8-75-00009 (1F)

SwRI Project No. 02-2332

Prepared for

National Aeronautics and Space Administration
George C. Marshall Space Flight Center
Huntsville, Alabama

2 June 1969

Approved:

H. Norman Abramson, Director
Department of Mechanical Sciences

PREFACE

This report constitutes the first of two volumes which summarize the work accomplished under Contract No. NAS8-21282. It includes supporting experimental data along with an analysis which is designed to predict natural frequencies and forced axisymmetric response in a vehicle propellant tank. The results are required for further analysis of dynamic stability, which has been accomplished in the second phase of the work under the above contract, and published in Final Report, Part II, entitled "Dynamic Stability of Cylindrical Propellant Tanks." The latter document includes a listing of a digital computer program developed to facilitate use of results from the entire research effort.

Both Part I and Part II of this Final Report are published on the same date. They present significant extensions and refinements of concepts originated under previous investigations conducted for NASA-MSFC. Results of this preliminary work are summarized in "Dynamic Stability and Parametric Resonance in Cylindrical Propellant Tanks," by Daniel D. Kana, Wen-Hwa Chu, and Tom D. Dunham, Final Report, Contract No. NAS8-20329, SwRI Project No. 02-1876, January 17, 1968.

ABSTRACT

The influence of a localized rigid mass has been determined for the longitudinal response of a model vehicle propellant tank. A theoretical analysis is conducted to predict the dynamic response of a simplified model consisting of a partially liquid filled cylinder which has a rigid flat bottom, an internal ullage pressure, and a rigid top mass. Donnell shell equations, along with additional terms to allow for geometrical nonlinearities, are used to determine natural frequencies and forced axisymmetric response of the model. Numerical results are compared with experimental observations for a range of several significant parameters. It is found that strong coupling occurs between the motion of the shell, liquid, and top mass over a wide portion of this range.

TABLE OF CONTENTS

PRINCIPAL NOTATION

a	radius of the shell
a_0	inner radius of the tank
c_0	speed of sound in the liquid
c_s	speed of stress waves in the shell, $(E/\rho_s)^{1/2}$
E	modulus of elasticity
f	excitation frequency in cps
g	standard acceleration of gravity
g_x	nondimensional excitation amplitude, $\hat{x}_0\omega^2/g$
H	nondimensional liquid depth, h/a
H_s	nondimensional thickness of shell, h_s/a
h	depth of liquid
h_s	thickness of shell
I_z	mass moment of inertia of top weight about z axis
ℓ	length of the shell
M	top mass
M_s	shell mass, $2\pi a h_s \ell \rho_s$
M**	nondimensional top mass
m	one-half of the number of circumferential nodes; $\cos(m\theta)$
$N_{xxs}, N_{\theta\theta s}, N_{x\theta s}$	static stress resultants
n	axial wave number, $\sin n\pi x/\ell$
P_r	nondimensional pressure loading on cylinder, p_r/E

p	pressure in the liquid
p_0	ullage pressure
p_r	pressure loading on the shell
P_{0n}^B	generalized loading due to bottom motion in a rigid tank
r, θ, x	cylindrical coordinates (space fixed)
t	time
U, V, W, X, Y	u, v, w, x, y, nondimensionalized by the radius a
u, v, w	displacements along x, θ, r direction, respectively
X_0	nondimensional amplitude of axial excitation, $X_0 = \hat{x}_0/a$
$x_0(t)$	excitation displacement
$\hat{x}_0$	displacement amplitude of axial excitation
λ	axial wavelength parameter, $n\pi a/\ell$
ν	Poisson's ratio
ρ	mass density of liquid
ρ_s	mass density of the shell
Ω	nondimensional frequency, $\omega a/c_s$
Ω_k	k-th eigenvalue, $\omega_k a/c_s$
ω	circular frequency of excitation

Superscripts and Subscripts

$( )^p$	related to the forced response
$(\hat{})$	the amplitude of ( )

LIST OF ILLUSTRATIONS

INTRODUCTION

The interaction of liquids and their elastic containers plays an important role in overall longitudinal response of launch vehicles since liquid pressures form complex effective masses, as well as avenues of energy feedback in a vehicle structure. As a result, synthesis of systems into relatively simple spring-mass representations[1] provides only a gross approximation of vehicle response, although such procedures are very useful from a design point of view.

Various types of responses which occur in a typical single propellant tank have been described by Kana and Gormley[2], while a membrane approach to axisymmetric responses has been given by Kana, et al.[3] Both of these articles contain substantial reference lists for additional studies which have been reported. All of these previous studies which include a more exact approach to the liquid-tank interaction problem have concerned only single propellant tank systems, although internal pressurization and elastic support effects were included.

The purpose of the present work is to extend the analysis of a single tank to include a rigid top mass, so that a better understanding can be obtained for the coupled effects which occur in an overall vehicle structure. Both symmetric and nonsymmetric responses are considered, although the latter are shown to be unaffected by the magnitude of the top mass. Symmetric responses are carefully considered, in view of their importance in spring-

mass model representations[1], as well as their formation of the parametric loadings for dynamic stability in liquid-tank systems[4].

It will be seen that the problem under concern is complicated by the fact that the eigenvalues appear in the boundary condition at the top of the tank for the case of symmetric responses. In order to handle this cumbersome feature, a technique which includes Fourier expansions combined with polynomial functions is utilized to produce a matrix-eigenvalue formulation.

THEORETICAL ANALYSIS

General

A schematic of the system to be investigated is shown in Figure 1, where some parameters are also given for the experimental apparatus. Thus, we consider a partially liquid filled thin cylindrical shell, which is internally pressurized, has a rigid flat bottom, and supports a rigid top mass. First, we consider the case of both symmetric and nonsymmetric free vibration, and then axisymmetric response to longitudinal excitation.

The governing shell equations for the present problem can be obtained from those developed by Sanders[5,6], after retaining only those terms which result from geometric nonlinearities. Thus, the effects of static stresses will be accounted for. The equations are

$$\frac{\partial^2 u}{\partial x^2} + \frac{\nu}{a}\frac{\partial^2 v}{\partial x \partial \theta} + \frac{\nu}{a}\frac{\partial w}{\partial x} + \frac{1-\nu}{2a^2}\left(\frac{\partial^2 u}{\partial \theta^2} + a\frac{\partial^2 v}{\partial x \partial \theta}\right) = \frac{1-\nu^2}{Eh_s}\left(\rho_s h_s \frac{\partial^2 u}{\partial t^2}\right) \quad (1a)$$

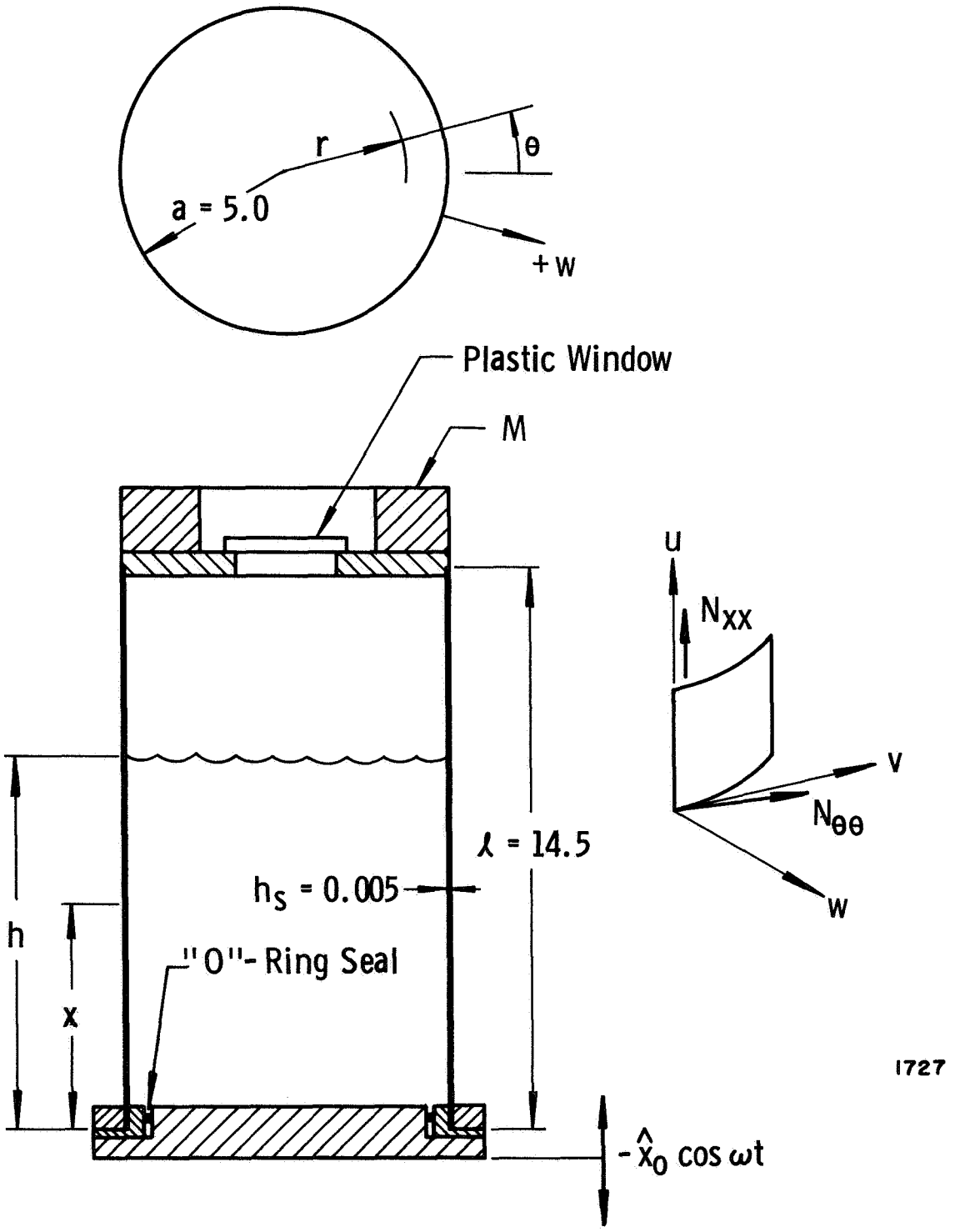

Figure 1. Coordinate System For Model

$$\frac{1}{a^2}\left[\frac{\partial^2 v}{\partial\theta^2}+\frac{\partial w}{\partial\theta}+a\nu\frac{\partial^2 u}{\partial x\partial\theta}+a^2\frac{(1-\nu)}{2}\left(\frac{\partial^2 v}{\partial x^2}+\frac{1}{a}\frac{\partial^2 u}{\partial x\partial\theta}\right)\right]$$

$$=\frac{(1-\nu^2)}{Eh_s}\left(\rho_s h_s\frac{\partial^2 v}{\partial t^2}\right) \qquad (1b)$$

$$\frac{1}{a}\left[\frac{1}{a}\frac{\partial v}{\partial\theta}+\frac{w}{a}+\nu\frac{\partial u}{\partial x}\right]+\frac{h_s^2}{12}\left[\frac{\partial^4 w}{\partial x^4}+\frac{2}{a^2}\frac{\partial^4 w}{\partial x^2\partial\theta^2}+\frac{1}{a^4}\frac{\partial^4 w}{\partial\theta^4}\right]$$

$$-\frac{1-\nu^2}{Eh_s}\left[\frac{\partial}{\partial x}\left(N_{xxs}\frac{\partial w}{\partial x}\right)+\frac{1}{a^2}\frac{\partial}{\partial\theta}\left(N_{\theta\theta s}\frac{\partial w}{\partial\theta}\right)+\frac{1}{a}\frac{\partial}{\partial x}\left(N_{x\theta s}\frac{\partial w}{\partial\theta}\right)\right.$$

$$\left.+\frac{1}{a}\frac{\partial}{\partial\theta}\left(N_{x\theta s}\frac{\partial w}{\partial x}\right)\right]=\frac{1-\nu^2}{Eh_s}\left(p_r-\rho_s h_s\frac{\partial^2 w}{\partial t^2}\right) \qquad (1c)$$

where N_{xxs}, $N_{x\theta s}$, $N_{\theta\theta s}$ are axisymmetric static stress resultants formed by internal pressurization, hydrostatic liquid pressure, and the static weight of the top mass.

Natural Frequencies of Partially-Filled Tank with Top Mass

This section deals with vibrational modes whose radial displacements are proportional to $\cos m\theta$. The case of axisymmetric vibration is contained as a special case with $m = 0$. Expanding the axial displacement into a Fourier cosine series in x plus a quadratic polynomial* to satisfy the two end conditions, and circumferential and radial displacements into Fourier sine series in x, there results:

---

*Note that this procedure is equivalent to expanding $\partial^2 U/\partial X^2$ into a Fourier cosine series.

$$U = \left[\frac{1}{2} B_2 X^2 + B_1 \left(X - \frac{\ell}{a}\right) + B_{m0} + \sum_{n=1}^{\infty} B_{mn} \cos\left(\frac{n\pi x}{\ell}\right)\right] \cos(m\theta) \cos(\omega t) \tag{2a}$$

$$V = \sum_{n=1}^{\infty} C_{mn} \sin\left(\frac{n\pi x}{\ell}\right) \sin(m\theta) \cos(\omega t) \qquad \begin{matrix} 0 \le x \le \ell \\ 0 \le \theta \le 2\pi \end{matrix} \tag{2b}$$

$$W = \sum_{n=1}^{\infty} A_{mn} \sin\left(\frac{n\pi x}{\ell}\right) \cos(m\theta) \cos(\omega t) \tag{2c}$$

The boundary conditions are:

- At $X = 0$:

$$U = 0, \quad W = 0, \quad V = 0 \quad , \quad \frac{\partial^2 W}{\partial X^2} = 0 \tag{3 a, b, c, d}$$

- At $X = \ell/a$:

$$\frac{\partial U}{\partial X} = M^{**}\Omega_k^2 U, \quad W = 0, \quad V = 0 \quad , \quad \frac{\partial^2 W}{\partial X^2} = 0 \tag{4 a,b, c, d}$$

where

$$M^{**} = \frac{M(1 - \nu^2)}{2\pi\rho_s a^3 H_s} \qquad \text{for } m = 0$$

$$M^{**} = \frac{1}{4} \frac{(1 - \nu 2)\, I_z}{\rho_s h_s a^5} \qquad \text{for } m = 1 \tag{5}$$

$$M^{**} = \infty \qquad \text{for } m \ge 2$$

Equations for determining the unknown coefficients in Equations (2) will now be formulated. To satisfy the boundary conditions on axial displacement, one has, from Equation (3a),

$$B_1 \frac{\ell}{a} - B_{m0} - \sum_{n=1}^{\infty} B_{mn} = 0 \tag{6}$$

Boundary condition (4a) requires

$$B_2\left(\frac{\ell}{a}\right)\left(\frac{1}{M^{**}}\right)+\frac{B_1}{M^{**}}-\Omega_k^2\left[\left(\frac{1}{2}\right)B_2\left(\frac{\ell}{a}\right)^2+B_{m0}+\sum_{n=1}^{\infty}B_{mn}(-1)^n\right]=0 \qquad (7a)$$

for $m = 0, 1$ or

$$\left(\frac{1}{2}\right)B_2\left(\frac{\ell}{a}\right)^2+B_{m0}+\sum_{n=1}^{\infty}B_{mn}(-1)^n=0 \qquad (7b)$$

for $m \geq 2$.

Upon substitution of Equations (2) into the axial equation of motion (1a), the x-independent Fourier coefficient ($n' = 0$) yields

$$-B_2\left[1-m^2\frac{(1-\nu)}{4}\chi_{20}\right]+m^2\frac{(1-\nu)}{2}\left(\chi_{10}-\frac{\ell}{a}\right)B_1+m^2\frac{(1-\nu)}{2}B_{m0}$$
$$-\Omega_k^2(1-\nu^2)\left[\left(\frac{1}{2}\right)B_2\chi_{20}+B_1\left(\chi_{10}-\frac{\ell}{a}\right)+B_{m0}\right]=0 \qquad (8)$$

where

$$\chi_{20}=\left(\frac{1}{3}\right)\left(\frac{\ell}{a}\right)^2 \quad , \quad \chi_{10}=\left(\frac{1}{2}\right)\left(\frac{\ell}{a}\right)$$

Similarly, for $n' > 1$, the $\cos(n'\pi x/\ell)$ coefficient of the axial Equation (1a) yields

$$\sum_{n=1}^{\infty}\left(\lambda_n^2+\frac{1-\nu}{2}m^2\right)B_{mn}\delta_{n'n}-\sum_{n=1}^{\infty}\frac{1+\nu}{2}m\lambda_nC_{mn}\delta_{n'n}$$
$$-\nu\sum_{n=1}^{\infty}\lambda_nA_{mn}\delta_{n'n}+m^2\frac{1-\nu}{2}\left(\frac{1}{2}B_2\chi_{2n'}+B_1\chi_{1n'}\right)$$
$$-(1-\nu^2)\Omega_k^2\left[\frac{1}{2}\chi_{2n'}B_2+\chi_{1n'}B_1+\sum_{n=1}^{\infty}B_{mn}\delta_{n'n}\right]=0 \qquad (9)$$

The $\sin(n'\pi x/\ell)$ coefficient of the circumferential Equation (1b) yields

$$\frac{1+\nu}{2} m \left(\tilde{\chi}_{1n'}B_2 + \tilde{\chi}_{0n'}B_1\right) - m \sum_{n=1}^{\infty} \frac{1+\nu}{2} \lambda_n \delta_{n'n} B_{mn}$$

$$+ \sum_{n=1}^{\infty} \left(\frac{1-\nu}{2} \lambda_n^2 + m^2\right) C_{mn}\delta_{n'n} + m \sum_{n=1}^{\infty} A_{mn}\delta_{n'n}$$

$$- (1-\nu^2)\Omega_k^2 \sum_{n=1}^{\infty} C_{mn}\delta_{n'n} = 0 \qquad (10)$$

The $\sin(n'\pi x/\ell)$ coefficient of the radial Equation (1c) yields

$$\nu\left(\tilde{\chi}_{1n'}B_2 + \tilde{\chi}_{0n'}B_1 - \sum_{n=1}^{\infty} \lambda_n \delta_{n'n} B_{mn}\right) + m \sum_{n=1}^{\infty} C_{mn}\delta_{n'n}$$

$$+ \sum_{n=1}^{\infty} \left\{\left[1 + \frac{H_s^2}{12}(\lambda_n^2 + m^2)^2\right] \delta_{n'n} + \frac{1-\nu^2}{H_s}\left[\frac{p_0}{2E}\lambda_n^2\right.\right.$$

$$\left.\left. - \frac{Mg\lambda_n^2}{2\pi a^2 E} + m^2 \frac{p_0}{E}\right] \delta_{n'n} + \frac{\rho g a}{E} m^2 \chi_{3n'n}\right\} A_{mn}$$

$$- (1-\nu^2)\Omega_k^2 \sum_{n=1}^{\infty} A_{mn}(\delta_{n'n} + M_{mn'n}) = 0 \qquad (11)$$

where, for Equations (9) through (11), we define

$$\lambda_n = \frac{n\pi a}{\ell} \quad , \quad \lambda_{n'} = \frac{n'\pi a}{\ell}$$

$$\tilde{\chi}_{1n'} = \frac{2a}{\ell} \int_0^{\ell/a} X \sin\left(\frac{n'\pi a}{\ell} X\right) dX \quad , \quad \tilde{\chi}_{0n'} = \frac{2a}{\ell} \int_0^{\ell/a} \sin\left(\frac{n'\pi a}{\ell} X\right) dX$$

$$\chi_{1n'} = \frac{2a}{\ell} \int_0^{\ell/a} X \cos\left(\frac{n'\pi a}{\ell} X\right) dX \quad , \quad \chi_{2n'} = \frac{2a}{\ell} \int_0^{\ell/a} X^2 \cos\left(\frac{n'\pi a}{\ell} X\right) dX$$

$$\chi_{3n'n} = \frac{2a}{\ell} \int_0^H (H - X) \sin(\lambda_n X) \sin(\lambda_{n'} X)\, dX$$

and, in Equation (1c), for the added mass pressure of the $\cos m\theta$ mode [obtained from Equations (18) in the next section] we have used

$$P_r = \sum_{n=1}^{\infty} \frac{p_{mn}}{E} = \sum_{n=1}^{\infty} \sum_{n'=1}^{\infty} H_s \Omega_k^2 A_{mn} M_{mn'n} \sin\left(\frac{n'\pi a}{\ell} X\right) \cos(m\theta)$$

Thus, in Equation (11), the effect of initial tension due to the ullage pressure, the hydrostatic pressure, and top weight are included in addition to that of the dynamic liquid pressure.

Equations (6) through (11) can be cast into the following matrix form:

$$\underbrace{\begin{bmatrix} [U_1] & [V_1] & [W_1] & \{0\} & \{Y_1\} & \{Z_1\} \\ [U_2] & [V_2] & [W_2] & \{0\} & \{Y_2\} & \{Z_2\} \\ [U_3] & [V_3] & [W_3] & \{0\} & \{Y_3\} & \{Z_3\} \\ (0) & (V_4) & (0) & X_4 & Y_4 & 0 \\ (0) & (V_5) & (0) & X_5 & Y_5 & Z_5 \\ (0) & (0) & (0) & X_6 & Y_6 & Z_6 \end{bmatrix}}_{3N+3 \times 3N+3} \underbrace{\begin{Bmatrix} \{A_{mn}\} \\ \{B_{mn}\} \\ \{C_{mn}\} \\ B_{m0} \\ B_1 \\ B_2 \end{Bmatrix}}_{3N+3 \times 1} - \tilde{\Omega}_k^2 \underbrace{\begin{bmatrix} [R_1] & [0] & [0] & \{0\} & \{0\} & \{0\} \\ [0] & [S_2] & [0] & \{0\} & \{P_2\} & \{Q_2\} \\ [0] & [0] & [T_3] & \{0\} & \{0\} & \{0\} \\ (0) & (0) & (0) & 0 & 0 & 0 \\ (0) & (S_5) & (0) & N_5 & 0 & Q_5 \\ (0) & (0) & (0) & N_6 & P_6 & Q_6 \end{bmatrix}}_{3N+3 \times 3N+3} \underbrace{\begin{Bmatrix} \{A_{mn}\} \\ \{B_{mn}\} \\ \{C_{mn}\} \\ B_{m0} \\ B_1 \\ B_2 \end{Bmatrix}}_{3N+3 \times 1} = 0 \quad (12)$$

where all series have been truncated to N-terms. To form Equation (12), we have written, respectively, Equations (11), (9), (10), (6), (7), and (8) in this order. Further,

$$\tilde{\Omega}_k^2 = (1 - \nu^2)\, \Omega_k^2$$

while [ ] designates a square $N \times N$ submatrix, $\{\ \}$ an $N \times 1$ column submatrix, ( ) a $1 \times N$ row submatrix, and all other elements are scalars.

Note that a [0] indicates a square submatrix whose elements are all zero, etc. Elements of all these submatrices are given in the Appendix. Submatrices of the $3N+3 \times 1$ column matrices are $N \times 1$ column matrices given by

$$\{A_m\} = \begin{Bmatrix} A_{m1} \\ A_{m2} \\ \vdots \\ A_{mN} \end{Bmatrix}, \quad \{B_m\} = \begin{Bmatrix} B_{m1} \\ B_{m2} \\ \vdots \\ B_{mN} \end{Bmatrix}, \quad \{C_m\} = \begin{Bmatrix} C_{m1} \\ C_{m2} \\ \vdots \\ C_{mN} \end{Bmatrix} \tag{12a}$$

Equation (12) can be expressed as

$$\left[[\![U]\!] - \tilde{\Omega}_k^2 [\![R]\!] \right] \{A\} = 0$$

Then, since $[\![R]\!]$ is a singular matrix, the eigenvalues and eigenvectors can be determined from a standard computer subroutine from

$$\left\{ [\![U]\!]^{-1} [\![R]\!] - \frac{1}{\tilde{\Omega}_k^2} [I] \right\} \{A\} = 0 \tag{13}$$

Thus, for the k, m-th natural frequency, the eigenvectors give the displacement components as

$$U_k = \left[\frac{1}{2} B_{2k} X^2 + B_{1k} \left(X - \frac{\ell}{a} \right) + B_{m0k} + \sum_{n=1}^{N} B_{mnk} \cos \left(\frac{n\pi x}{\ell} \right) \right] \cos m\theta$$

$$V_k = \sum_{n=1}^{N} C_{mnk} \sin \left(\frac{n\pi x}{\ell} \right) \sin m\theta$$

$$W_k = \sum_{n=1}^{N} A_{mnk} \sin \left(\frac{n\pi x}{\ell} \right) \cos m\theta$$

Generalized Added Mass of Liquid

For radial shell vibrations that are proportional to $\cos m\theta$, the liquid exerts a radial pressure which may be regarded as an apparent mass $M_{mn'n}$ which is added to the cylinder mass. We now derive an expression for this quantity.

The fluid is assumed to be nonviscous, irrotational, but compressible. The velocity potential corresponding to the mn-th component of shell motion for small disturbances is governed by the wave equation which for periodic motion is

$$\nabla^2\phi_{mn} + \frac{\omega^2}{c_0^2}\phi_{mn} = 0$$

The boundary condition on the wall is

$$\frac{\partial\phi_{mn}}{\partial r} = \frac{\partial w_{mn}}{\partial t} \quad \text{at} \quad r = a \ (w_{mn} \text{ outward positive}) \tag{14}$$

where the mn-th component of radial shell motion is

$$w_{mn} = \tilde{A}_{mn}(t) f_n(x) \cos(m\theta) \tag{15}$$

and we assume that $f_n(x)$ is an orthogonal set of functions in the interval $[0, \ell]$. The boundary condition at the bottom is:

$$\frac{\partial\phi_{mn}}{\partial x} = 0 \quad \text{at} \quad x = 0 \tag{16}$$

When frequency of excitation is much higher than the leading few liquid surface sloshing frequencies in consideration, the free surface condition can be approximated by

$$\phi_{mn} = 0 \quad \text{at} \quad x = h \tag{17}$$

By separation of variables, a particular solution can be constructed to satisfy the boundary conditions on the wetted surface [Eqs. (14) and (16)] as:

$$\phi_1 = \sum_{k=0}^{\infty} D_{kn} R_{mk} \left(\frac{r}{a}, \omega\right) \cos\left(\frac{k\pi x}{h}\right) \cos(m\theta) \left(a \frac{d\tilde{A}_{mn}}{dt}\right)$$

with Fourier expansion of $f_n(x)$ being

$$f_n(x) = \sum_{k=0}^{\infty} D_{kn} \cos\left(\frac{k\pi x}{h}\right)$$

where

$$D_{kn} = \int_0^h f_n(x) \cos\left(\frac{k\pi x}{h}\right) dx \cdot \frac{2}{1+\delta_{0n}}$$

and

$$R_{mk} = \frac{I_m\left(\xi_k \frac{r}{a}\right)}{\xi_k I'_m(\xi_k)} \quad \text{for} \quad k \geq \frac{\omega h}{\pi c_0}$$

$$R_{mk} = \frac{J_m\left(\xi_k \frac{r}{a}\right)}{\xi_k J'_m(\xi_k)} \quad \text{for} \quad k \leq \frac{\omega h}{\pi c_0}$$

where

$$\xi_k = \left[\left|\left(\frac{k\pi a}{h}\right)^2 - \frac{\omega^2 a^2}{c_0^2}\right|\right]^{\frac{1}{2}}$$

Next consider a complementary solution, satisfying homogeneous boundary conditions on the wetted surfaces so that the net velocity potential satisfies the approximate free-surface condition:

$$\phi_2 = \left[\sum_{j=1}^{\infty} \tilde{B}_{mjn} J_m\left(\mu_{mj} \frac{r}{a}\right) C_j\left(\frac{x}{a}, \omega\right) \cos(m\theta) + \right.$$

$$\left. + \delta_{m0} \tilde{B}_{00n} \cos\left(\frac{\omega a}{c_0} \frac{x}{a}\right)\right]\left(-a \frac{d\tilde{A}_{mn}}{dt}\right)$$

where

μ_{mj} is the j-th root of $J'_m(\mu_{mj}) = 0$

$$C_j\left(\frac{x}{a},\omega\right) = \cosh\left(\eta_{mj}\frac{x}{a}\right) \quad \text{for} \quad \mu_{mj} \geq \frac{\omega a}{c_0}$$

and

$$C_j\left(\frac{x}{a},\omega\right) = \cos\left(\eta_{mj}\frac{x}{a}\right) \quad \text{for} \quad \mu_{mj} < \frac{\omega a}{c_0}$$

where

$$\eta_{mj} = \left[\left|\mu_{mj}^2 - \frac{\omega^2 a^2}{c_0^2}\right|\right]^{\frac{1}{2}}$$

$$E_{kj} = \frac{\int_0^1 \frac{r}{a} R_{mk}\left(\frac{r}{a},\omega\right) J_m\left(\mu_{mj}\frac{r}{a}\right) d\left(\frac{r}{a}\right)}{\int_0^1 \frac{r}{a} J_m^2\left(\mu_{mj}\frac{r}{a}\right) d\left(\frac{r}{a}\right)}$$

$$E_{k0} = 2\int_0^1 \frac{r}{a} R_{0k}\left(\frac{r}{a},\omega\right) d\left(\frac{r}{a}\right)$$

$$\tilde{B}_{mjn} = \frac{\sum_{k=0}^{\infty} (-1)^k D_{kn} E_{kj}}{C_j\left(\frac{h}{a},\omega\right)}$$

$$\tilde{B}_{00n} = \frac{\sum_{k=0}^{\infty} (-1)^k D_{kn} E_{k0}}{\cos\left(\frac{\omega h}{c_0}\right)}$$

The total velocity potential is given by

$$\phi_{mn} = \phi_1 + \phi_2$$

and the linearized pressure loading, given by the Bernoulli equation, is

$$p_{mn} = -\rho \left.\frac{\partial \phi_{mn}}{\partial t}\right|_{r=a}$$

As a result, the n'-th component of generalized force $p_{mn'n}$ is given by integration of the loading with a weighting function $f_{n'}(x)$:

$$p_{mn'n} = \frac{\int_0^{\ell} f_{n'}(x)\, p_{mn}\, dx}{\int_0^{\ell} f_{n'}^2(x)\, dx} = -M_{mn'n}\rho_s h_s \cos m\theta \frac{d^2\tilde{A}_{mn}}{dt^2}$$

where the generalized apparent mass is

$$M_{mn'n} = \frac{\rho a}{\rho_s h_s}\left\{ \sum_{k=1}^{\infty} R_{mk}(1,\omega)\, D_{kn}\tilde{D}_{kn'} \right.$$

$$-\left[\sum_{k=1}^{\infty} E_{k0} D_{kn} (-1)^k \tilde{E}_{n'}\delta_{0m} \Big/ \cos\left(\frac{\omega h}{c_0}\right)\right] + \left[\frac{2}{\xi_0^2} \frac{\tilde{\tilde{E}}_{n'}}{\cos\frac{\omega h}{c_0}}\right.$$

$$\left.\left. - \frac{J_0(\xi_0)}{\xi_0 J_1(\xi_0)} \tilde{D}_{0n'}\right] D_{0n}\delta_{m0} + (1 - \delta_{m0}) \left[D_{0n}\tilde{D}_{0n'} \cdot \frac{J_m(\xi_0)}{\xi_0 J_m'(\xi_0)}\right]\right.$$

$$\left. - \sum_{j=1}^{\infty} J_m(\mu_{mj})\, \tilde{C}_{nj}\tilde{B}_{mjn} \right\} \qquad (18a)$$

in which

$$\tilde{D}_{kn'} = \frac{\int_0^{h} \cos\left(\frac{k\pi x}{h}\right) f_{n'}(x)\, dx}{\int_0^{\ell} f_{n'}^2(x)\, dx}$$

$$\tilde{C}_{n'j} = \frac{\int_0^h C_j\left(\frac{x}{a}, \omega\right) f_{n'}(x)\, dx}{\int_0^\ell f_{n'}^2(x)\, dx}$$

$$\tilde{E}_{n'} = \frac{\int_0^h \cos\left(\frac{\omega x}{c_0}\right) f_{n'}(x)\, dx}{\int_0^\ell f_{n'}^2(x)\, dx} = \tilde{D}_{0n'}$$

Note then that the mn-th component of pressure loading on the shell is

$$p_{mn} = \sum_{n'=1}^{\infty} p_{mn'n} f_{n'}(x) = -\sum_{n'=1}^{\infty} \rho_s h_s M_{mn'n} \cos(m\theta) f_{n'}(x) \frac{d^2\tilde{A}_{mn}}{dt^2} \tag{18b}$$

Thus, $M_{mn'n}$ is the coefficient of $\rho_s h_s (d^2/dt^2)(\tilde{A}_{mn})$ in the n'-th component of shell motion exhibiting a $\cos(m\theta)$ mode of vibration. To use this generalized coefficient in Equation (11), we note from Equation (2c) that $f_{n'}(x)$ assumes the form

$$f_{n'}(x) = \sin\left(\frac{n'\pi x}{\ell}\right)$$

Forced Axisymmetric Response

Now, assume the tank is excited axially. A similar Fourier process will be utilized for the solution of this case, so that the same shell displacement forms [Eqs. (2)] are again used, except that a superscript p will be incorporated to designate the forced motion. Further, the response will occur at the excitation frequency Ω, rather than at a natural frequency Ω_k. Finally, in this section we discuss only axisymmetric motion (m = 0), which is of the most practical concern in a linear formulation.

The boundary conditions on axial displacement become

$$\text{At } X = 0 \quad , \quad U = -X_0 \cos(\omega t) \tag{19}$$

$$\text{At } X = \frac{\ell}{a} \quad , \quad \frac{\partial U}{\partial X} = M^{**}\Omega^2 U \tag{20}$$

To satisfy Equation (19), one has, from Equation (2a):

$$B_1^p \frac{\ell}{a} - B_{m0}^p - \sum_{n=1}^{\infty} B_{mn}^p = X_0$$

Additional equations corresponding to Equations (7a), (8), (9), and (10) can now be written as before. For brevity we do not write these equations since they are identical to those mentioned except that the coefficients carry the superscript p and Ω replaces Ω_k. Finally, an equation corresponding to (11) can also be written for the forced response. However, we must first discuss the difference in pressure loading that will occur.

As a result of the axial motion of the tank bottom, the liquid exerts a generalized radial pressure loading p_{0n}^B on the tank wall in addition to the apparent mass pressure p_{mn}^p. That is, for forced motion the total pressure can be expressed as

$$p_r^p = p_{mn}^p + p_{0n}^B \tag{21}$$

The apparent mass pressure p_{mn}^p has already been determined by Equation (18b) providing that $\tilde{A}_{mn}^p$ is utilized in lieu of $\tilde{A}_{mn}$. The additional pressure loading p_{0n}^B remains to be determined. This pressure can be derived from a one-dimensional velocity potential which satisfies the wave equation along with the boundary conditions:

$$\phi^B = 0 \quad \text{at} \quad x = h$$

$$\frac{\partial \phi^B}{\partial x} = \hat{x}_0 \omega \sin \omega t \quad \text{at} \quad x = 0$$

The velocity potential which satisfies these conditions can be found as

$$\phi^B = \frac{-\omega \hat{x}_0 \sin \omega t \sin \left[\frac{\omega}{c_0}(h - x)\right]}{\frac{\omega}{c_0} \cos\left(\frac{\omega h}{c_0}\right)}$$

Thus, the generalized loading (which results from the application of the Fourier process) relative to the n'-th tank-displacement component can be expressed as:

$$P^B_{0n'} = \frac{p^B_{0n}}{EH_s} = \frac{1}{a^2_{n'}} \int_0^h \frac{\rho \omega^2 \hat{x}_0 \cos(\omega t) \sin\left(\frac{\omega}{c_0}(h - x)\right) f_{n'}(X)}{EH_s \frac{\omega}{c_0} \cos\left(\frac{\omega h}{c_0}\right)} \frac{dx}{a}$$

where

$$a^2_{n'} = \frac{1}{2} \frac{\ell}{a}$$

The amplitude of this loading becomes

$$\hat{P}^B_{0n'} = \frac{\rho a}{\rho_s h_s} \Omega \cdot \left(\frac{c_0}{c_s}\right) \frac{I_{0n'}}{\cos\left(\Omega H \frac{c_s}{c_0}\right)} \tag{22}$$

where we define

$$I_{0n'} = \frac{1}{a^2_{n'}} \int_0^H \sin\left[\frac{\omega a}{c_0}(H - X)\right] \sin(\lambda_{n'} X)\, dX$$

We now are in position to formulate the last equation required for the solution of the forced response. Combining Equations (18b), (21), and (22), along with Equations (2) with superscripts p on the coefficients, into Equation (1c), and collecting the coefficients of the $\sin(n'\pi x/\ell)$ terms, there results

$$\nu\left[B_2^p\tilde{\chi}_{1n'} + B_1^p\tilde{\chi}_{0n'} - \sum_{n=1}^{\infty}\lambda_n B_{mn}^p\delta_{n'n}\right] + m\sum_{n=1}^{\infty}C_{mn}^p\delta_{n'n}$$

$$+\sum_{n=1}^{\infty}A_{mn}^p\delta_{n'n}\left\{1+\frac{H_s^2}{12}(\lambda_n^2+m^2)^2+\frac{1-\nu^2}{H_s}\left[\lambda_n^2\left(\frac{p_0}{2E}-\frac{Mg}{2\pi a^2E}\right)\right.\right.$$

$$\left.\left.+m^2\frac{p_0}{E}\right]\right\}+\frac{1-\nu^2}{H_s}m^2\sum_{n=1}^{\infty}\frac{\rho ga}{E}\chi_{3n'n}A_{mn}^p$$

$$-(1-\nu^2)\Omega^2\sum_{n=1}^{\infty}A_{mn}^p\left[\delta_{n'n}+M_{mn'n}\right]=(1-\nu^2)\hat{P}_{0n'}^B \qquad (23)$$

The equations for determining the forced response can now be put in the following matrix form

$$\left[[\![U]\!]-\tilde{\Omega}^2[\![R]\!]\right]\times\begin{Bmatrix}\{A_{mn}^p\}\\ \{B_{mn}^p\}\\ \{C_{mn}^p\}\\ B_{m0}^p\\ B_1^p\\ B_2^p\end{Bmatrix}=X_0\begin{Bmatrix}\{F_r\}\\ \{0\}\\ \{0\}\\ 1\\ 0\\ 0\end{Bmatrix} \qquad (24)$$

where

$$\tilde{\Omega}^2=(1-\nu^2)\Omega^2$$

and the elements of the $\{F_r\}$ matrix are

$$F_{rn'} = (1 - \nu^2)\,\hat{P}^B_{0n'}$$

The $[\![U]\!]$ and $[\![R]\!]$ matrices are the same as in Equation (12). Here, however, the column matrices of response coefficients are different from those of the natural modes.

For given values of X_0 and Ω, one can solve for the forced response by the following inversion:

$$\begin{Bmatrix} \{A^p_{mn}\} \\ \{B^p_{mn}\} \\ \{C^p_{mn}\} \\ B^p_{m0} \\ B^p_1 \\ B^p_2 \end{Bmatrix} = X_0 \left[[\![U]\!] - \tilde{\Omega}^2 [\![R]\!] \right]^{-1} \begin{Bmatrix} \{F_r\} \\ \{0\} \\ \{0\} \\ 1 \\ 0 \\ 0 \end{Bmatrix} \tag{25}$$

THEORETICAL AND EXPERIMENTAL RESULTS

Figure 2 shows the variation of natural frequency with liquid depth for several modes of a steel tank whose geometry is given in Figure 1. Each of the three parts of Figure 2 is for a different top mass. Theoretical computations were performed for the largest mass (Fig. 2a) only. All symmetric modes in the given frequency range were obtained, although only one nonsymmetric mode is indicated. Of course, many other nonsymmetric natural modes existed in this range (note that experimental data for two nonsymmetric modes are given in Figures 2b, c).

Natural frequencies for the symmetric modes were determined experimentally by detecting peaks in the pressure at the center of the tank bottom and/or detecting peaks in the output acceleration of the top mass. Although Figure 2 indicates a condition of zero ullage pressure, up to $p_0 =$ 10 psig had to be used in order to obtain data for the symmetric modes. This was necessary to prevent the occurrence of instability in some nonsymmetric mode, in which a simple linear symmetric response no longer was present. Fortunately, this procedure was possible since the frequencies of symmetric modes were determined to be independent of ullage pressure. We emphasize, however, that frequencies of nonsymmetric modes are highly dependent on ullage pressure, so that data for the $k = 1$, $m = 10$ mode (as well as the $k = 1$, $m = 13$ mode) in Figure 2 were taken at $p_0 = 0$. Data for these modes were

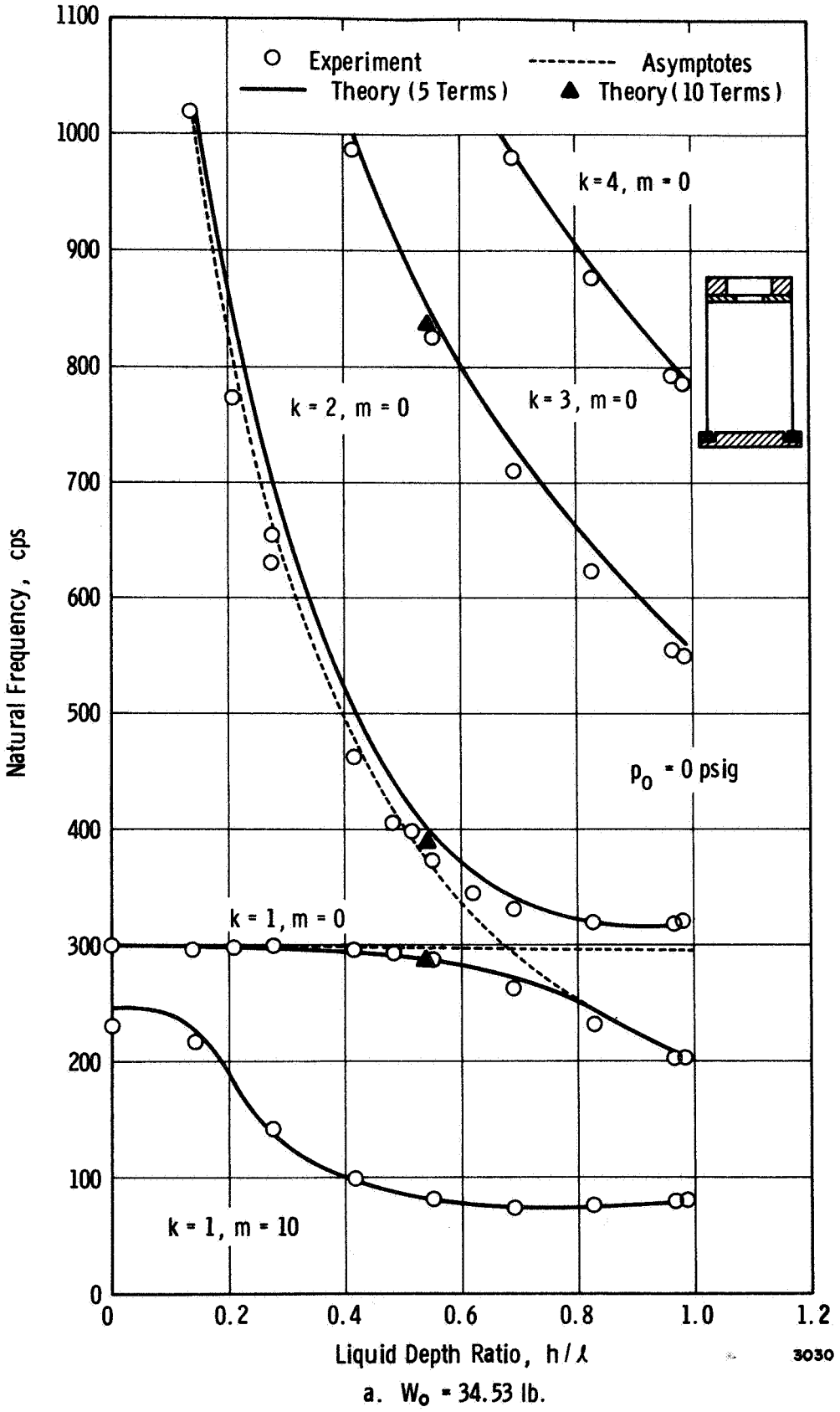

a. W_o = 34.53 lb.

Figure 2. Natural Frequencies Of Partially Filled Tank With Top Mass

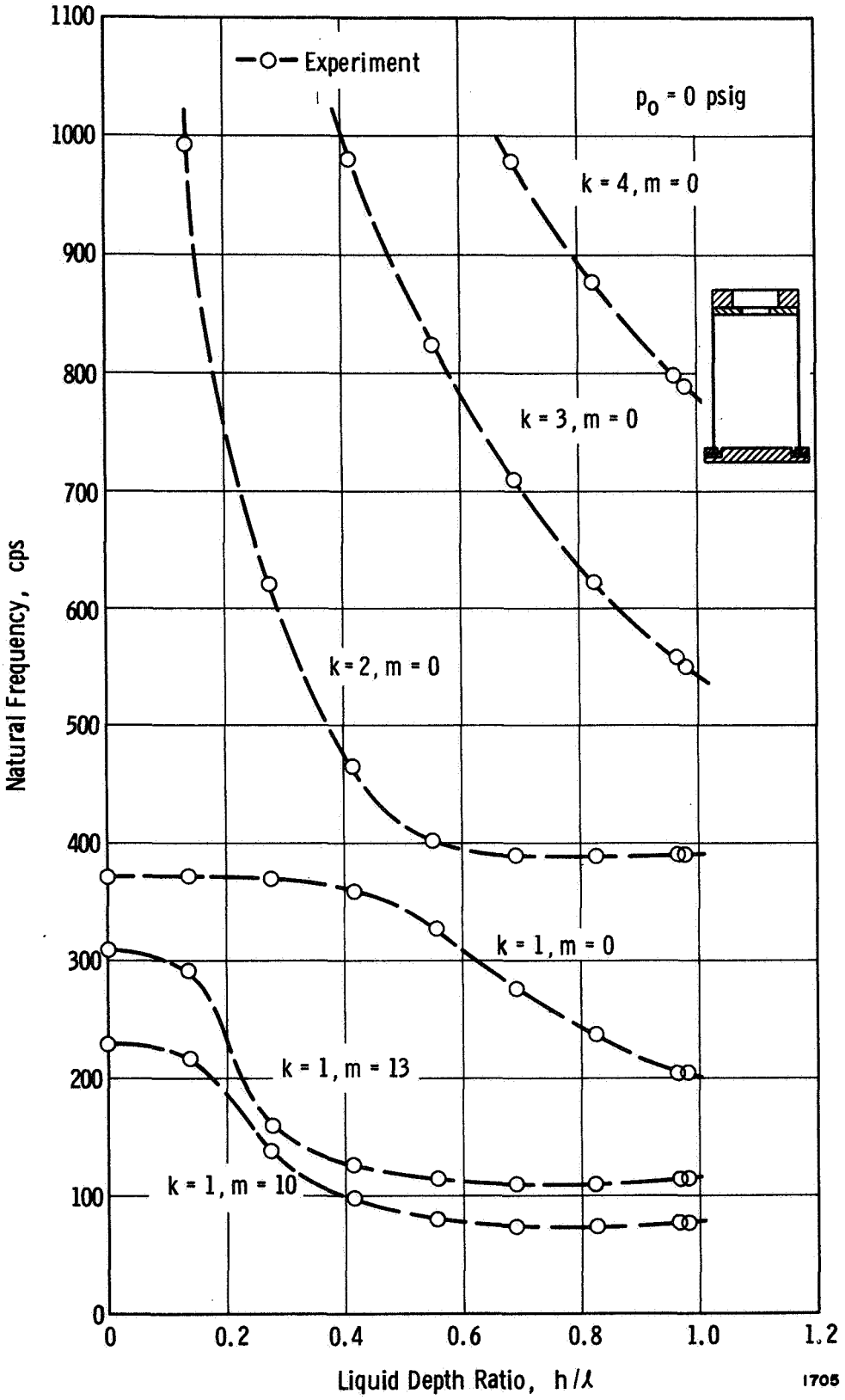

b. W_0 = 22.32 lb.

Figure 2. Natural Frequencies Of Partially Filled Tank With Top Mass

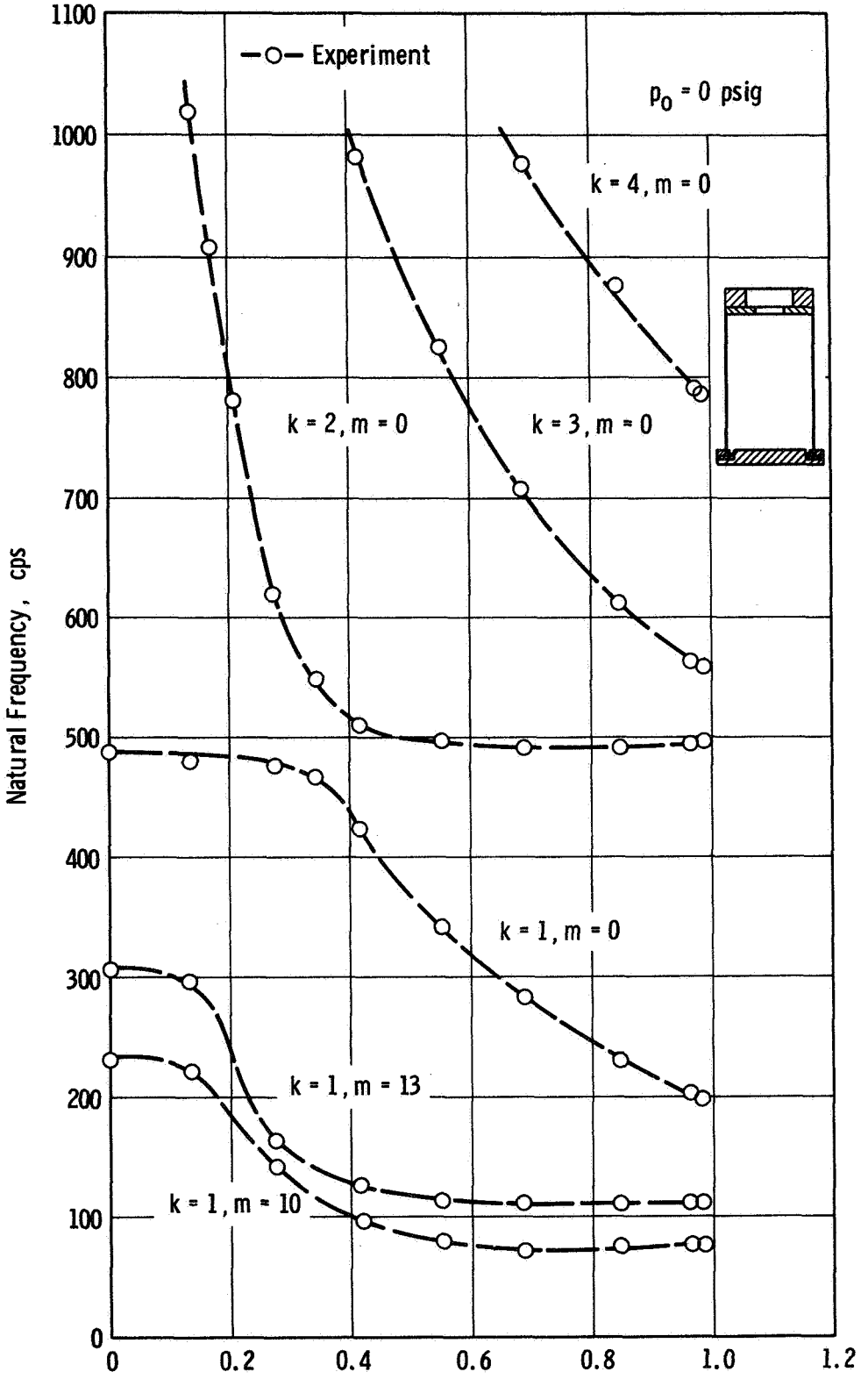

c. W_0 = 11.48 lb.

Figure 2. Natural Frequencies Of Partially Filled Tank With Top Mass

taken as peaks in the wall response at the antinode of the axial wave form. Of course, the position of this antinode shifted with different liquid depths.

Theoretical data for Figure 2a were obtained by the use of a five-term (n = 1 to 5) expansion in Equation (13) and computing the eigenvalue for the resulting 18 × 18 matrix. Some deviation between theory and experiment can be seen to exist in Figure 2a. However, the use of more terms in the expansions would reduce this deviation. This can be seen from the three points computed for n = 10 terms for the first three symmetric modes at a depth of $h/\ell = 0.55$. Since the five-term expansions appeared to give a sufficiently good comparions between theoretical and experimental results, most of the computations were thereby limited in order to reduce the required digital computer time.

Several interesting observations can be made from the data in Figure 2. Although the frequency of the m = 10 mode is considerably below those of the symmetric modes throughout most of the depth range, pressurizing the tank can raise the nonsymmetric mode above the lowest symmetric mode. For low liquid depths, it can be seen that the first symmetric mode represents the first coupled axial top mass-shell mode with only small liquid effects, while the second symmetric mode represents the first coupled liquid-shell mode with only small top-mass effects. However, these roles

of the first two modes are interchanged for greater liquid depths as indicated by the dashed lines in Figure 2a which represent the respective decoupled modes.

From Figure 2 it can be seen that variation in top mass had no effect on the nonsymmetric mode but a strong effect on the first two symmetric modes for a middepth range of liquid. This is shown further in Figure 3. Finally, the influence of ullage pressure on frequencies of the nonsymmetric linear mode was not measured since this has been determined by various previous investigations.

Figure 4 shows a comparison of theoretical and experimental axisymmetric forced response for a frequency range which includes the first two modes with a liquid depth of $h/\ell = 0.69$. Although the data were taken at $p_0 = 10$ psig, the results are independent of pressure, as has already been mentioned. Here, the acceleration amplification of the top mass was chosen as a comparison parameter, although the liquid pressure at some point in the tank could have been used just as well. An intermediate liquid depth was chosen as a worst possible condition for using a given number of series terms in the theoretical computations. That is, previous work indicates that the most serious distortions of tank axial mode shape from a half-sine wave occurs at intermediate depth ranges.

Theoretical points were determined from Equation (25) by means of a digital computer. Of course, the net sum of the forced

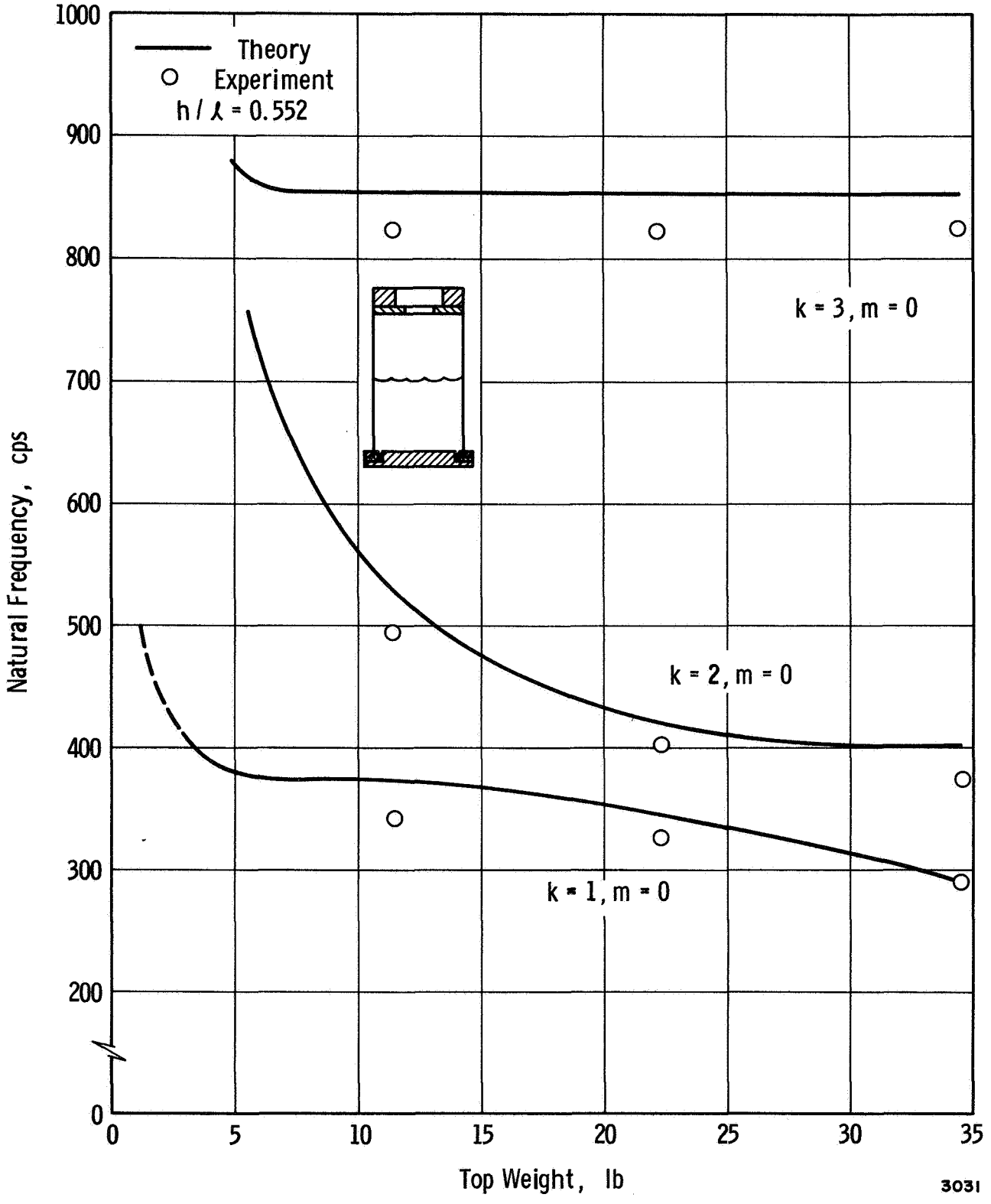

Figure 3. Effect Of Top Mass On Natural Frequencies

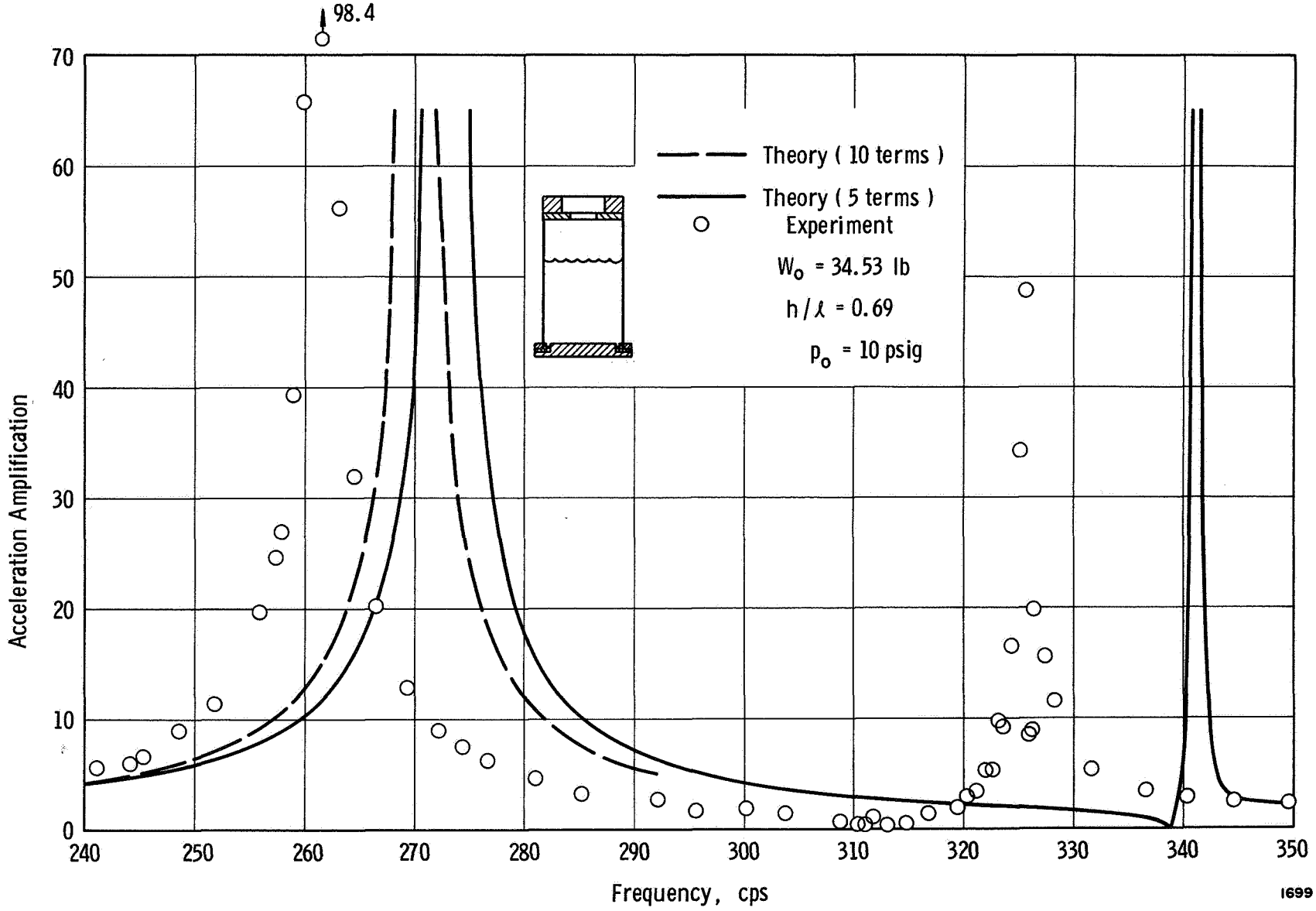

Figure 4. Response Of Top Mass Relative To Input Acceleration For Axisymmetric Wall Response

axial displacement components $\hat{u}$ at $x = \ell$ form the part of the theoretical solution which is used in Figure 4. Basically, five terms were used, although ten terms were used for part of the range as indicated. It can be seen that more terms reduce the discrepancy between theory and experiment. Also, the location of the theoretical and experimental resonance points corresponds with the location of the respective natural frequencies for the first two symmetric modes in Figure 2a. Thus, the agreement between theory and experiment can be made as good as is desired, and the most terms in the expansions are required at intermediate depths.

A final comment may be made with regard to the use of polynomial functions in conjunction with a Fourier series (see Eq. 2a). It is recognized that convergence of the solution may be of some concern. However, the relatively good comparison between experimental and theoretical results tends to refute the latter concern, at least in the range of parameters investigated.

ACKNOWLEDGMENTS

The authors wish to express their sincere appreciation to several colleagues for assistance during the conduct of this research program. Particular mention should be given to Dr. H. Norman Abramson for his counsel, to Mr. Dennis Scheidt for performing most of the experiments, to Mr. Robert Gonzales for digital computer programming, and to Mr. Victoriano Hernandez for preparing the figures in this report.

REFERENCES

1. Pinson, L. D., Leonard, H. W., and Raney, J. P., "Analyses of Longitudinal Dynamics of Launch Vehicles with Application to a 1/10-Scale Saturn V Model," AIAA Journal of Spacecraft and Rockets, Vol. 5, No. 3, March 1968, pp. 303-308.

2. Kana, D. D., and Gormley, J. F., "Longitudinal Vibration of a Model Space Vehicle Propellant Tank," AIAA Journal of Spacecraft and Rockets, Vol. 4, No. 12, December 1967, pp. 1585-1591.

3. Kana, D. D., Glaser, R. F., Eulitz, W. R., and Abramson, H. N., "Longitudinal Vibration of Spring-Supported Cylindrical Membrane Shells Containing Liquid," AIAA Journal of Spacecraft and Rockets, Vol. 5, No. 2, February 1968, pp. 189-196.

4. Kana, D. D., and Craig, R. R., Jr., "Parametric Oscillations of a Longitudinally Excited Cylindrical Shell Containing Liquid," AIAA Journal of Spacecraft and Rockets, Vol. 5, No. 1, January 1968, pp. 13-21

5. Sanders, J. L., Jr., "Nonlinear Theories for Thin Shells," Q. Appl. Math., Vol. XXI, No. 1, (1963), pp. 21-36.

6. Sanders, J. L., Jr., "An Improved First Approximation Theory for Thin Shells," NASA Rept. 24, June 1959.

APPENDIX

Elements of Submatrices in Equation (12)

n' designates row and n designates column of the respective elements

$$U_{1n'n} = \left[1 + \frac{H_s^2}{12}(\lambda_n^2 + m^2)^2\right]\delta_{n'n}$$

$$+ \frac{1 - \nu^2}{H_s}\left[\frac{p_0}{E}\left(\frac{\lambda_n^2}{2} + m^2\right)\delta_{n'n} - \frac{Mg\lambda_n^2}{2\pi a^2 E}\delta_{n'n} + \frac{\rho g a}{E} m^2 \chi_{3n'n}\right]$$

$$V_{1n'n} = -\lambda_n \nu \delta_{n'n} \quad , \quad W_{1n'n} = m\delta_{n'n}$$

$$Y_{1n'} = \nu\tilde{\chi}_{0n'} \quad , \quad Z_{1n'} = \nu\tilde{\chi}_{1n'} \quad , \quad R_{1n'n} = \delta_{n'n} + M_{mn'n}$$

$$U_{2n'n} = -\nu\lambda_n\delta_{n'n} \quad , \quad V_{2n'n} = \left[\lambda_n^2 + m^2\frac{(1 - \nu)}{2}\right]\delta_{n'n}$$

$$W_{2n'n} = -m\lambda_n\delta_{n'n}\frac{(1 + \nu)}{2} \quad , \quad Y_{2n'} = m^2\chi_{1n'}\frac{(1 - \nu)}{2}$$

$$Z_{2n'} = m^2\chi_{2n'}\frac{(1 - \nu)}{4} \quad , \quad S_{2n'n} = \delta_{n'n}$$

$$P_{2n'} = \chi_{1n'} \quad , \quad Q_{2n'} = \frac{\chi_{2n'}}{2}$$

$$U_{3n'n} = m\delta_{n'n} \quad , \quad V_{3n'n} = -m\lambda_n\delta_{n'n}\frac{(1 + \nu)}{2}$$

$$W_{3n'n} = \left[m^2 + \lambda_n^2\frac{(1 - \nu)}{2}\right]\delta_{n'n} \quad , \quad Y_{3n'} = m\tilde{\chi}_{0n'}\frac{(1 + \nu)}{2}$$

$$Z_{3n'} = m\tilde{\chi}_{1n'}\frac{(1 + \nu)}{2} \quad , \quad T_{3n'n} = \delta_{n'n}$$